International Journal of Radiation Oncology biology • physics

www.redjournal.org

Biology Contribution

A Comparative Study of the Hypoxia PET Tracers [^{18}F]HX4, [^{18}F]FAZA, and [^{18}F]FMISO in a Preclinical Tumor Model

Sarah G.J.A. Peeters, MSc,* Catharina M.L. Zegers, MSc,* Natasja G. Lieuwes, BSc,* Wouter van Elmpt, PhD,* Jonas Eriksson, PhD,† Guus A.M.S. van Dongen, PhD,† Ludwig Dubois, PhD,* and Philippe Lambin, MD, PhD*

**Department of Radiation Oncology, GROW - School for Oncology and Developmental Biology, Maastricht University Medical Centre, Maastricht, The Netherlands; and †Department of Radiology and Nuclear Medicine, VU University Medical Center Amsterdam, Amsterdam, The Netherlands*

Received Jun 13, 2014, and in revised form Sep 15, 2014. Accepted for publication Sep 30, 2014.

Summary

Visualizing hypoxic tumor regions is important for improving cancer treatment, and hypoxia positron emission tomography has been shown to be a promising tool. The tumor uptake of 3 clinical hypoxia PET tracers, [^{18}F]FMISO, [^{18}F]FAZA, and [^{18}F]HX4, was assessed in a preclinical tumor model to compare their performances regarding optimal imaging time, tumor-to-background ratios, spatial reproducibility, and modified

Purpose: Several individual clinical and preclinical studies have shown the possibility of evaluating tumor hypoxia by using noninvasive positron emission tomography (PET). The current study compared 3 hypoxia PET tracers frequently used in the clinic, [^{18}F]FMISO, [^{18}F]FAZA, and [^{18}F]HX4, in a preclinical tumor model. Tracer uptake was evaluated for the optimal time point for imaging, tumor-to-blood ratios (TBR), spatial reproducibility, and sensitivity to oxygen modification.

Methods and Materials: PET/computed tomography (CT) images of rhabdomyosarcoma R1-bearing WAG/Rij rats were acquired at multiple time points post injection (p.i.) with one of the hypoxia tracers. TBR values were calculated, and reproducibility was investigated by voxel-to-voxel analysis, represented as correlation coefficients (R) or Dice similarity coefficient of the high-uptake volume. Tumor oxygen modifications were induced by exposure to either carbogen/nicotinamide treatment or 7% oxygen breathing.

Results: TBR was stabilized and maximal at 2 hours p.i. for [^{18}F]FAZA (4.0 $\pm$ 0.5) and at 3 hours p.i. for [^{18}F]HX4 (7.2 $\pm$ 0.7), whereas [^{18}F]FMISO showed a constant increasing TBR (9.0 $\pm$ 0.8 at 6 hours p.i.). High spatial reproducibility was observed by voxel-to-voxel comparisons and Dice similarity coefficient calculations on the 30%

Reprint requests to: Sarah G.J.A. Peeters, MSc, Department of Radiation Oncology (MaastRO Lab), GROW - School for Oncology and Developmental Biology, Maastricht University Medical Centre, UNS 50/23 PO Box 616, 6200 MD Maastricht, The Netherlands. Tel: 31 (0)43 388-2908; E-mail: sarah.peeters@maastrichtuniversity.nl

This study was supported by Center for Translational Molecular Medicine framework 030-103 (Airforce), European Union seventh framework programmes (Metoxia grant agreement 222741 and Artforce grant agreement 257144), and the Kankeronderzoekfonds Limburg from the Health Foundation Limburg (Star project 2013).

Conflict of interest: none.

L. Dubois and P. Lambin contributed equally to this work.

Supplementary material for this article can be found at www.redjournal.org.

Int J Radiation Oncol Biol Phys, Vol. 91, No. 2, pp. 351–359, 2015

http://dx.doi.org/10.1016/j.ijrobp.2014.09.045

oxygen concentrations. This study provides insights into the strengths and weaknesses of these tracers.

highest uptake volume for both [^{18}F]FMISO (R = 0.86; Dice coefficient = 0.76) and [^{18}F]HX4 (R = 0.76; Dice coefficient = 0.70), whereas [^{18}F]FAZA was less reproducible (R = 0.52; Dice coefficient = 0.49). Modifying the hypoxic fraction resulted in enhanced mean standardized uptake values for both [^{18}F]HX4 and [^{18}F]FAZA upon 7% oxygen breathing. Only [^{18}F]FMISO uptake was found to be reversible upon exposure to nicotinamide and carbogen.

Conclusions: This study indicates that each tracer has its own strengths and, depending on the question to be answered, a different tracer can be put forward.

Introduction

Tumor hypoxia is an important factor in worsening cancer patients' treatment outcome. Regions of low oxygen concentration are a well-known characteristic of solid tumors and can be caused by impaired blood vessel development, temporal occlusions of blood vessels, or excessive tumor growth (1, 2). Knowledge of the extension and location of hypoxia would provide additional information that could be integrated into strategies of conventional treatments, potentially leading to improved therapeutic outcome (3). Positron emission tomography (PET) has been shown to be a suitable, noninvasive, 3-dimensional imaging technique for the detection of hypoxic tumor regions. PET tracers containing the oxygen-sensitive nitroimidazole group are specifically designed to detect hypoxic regions, and the feasibility of these tracers has been studied extensively in several independent clinical and preclinical studies (1).

^{18}F-labeled fluoromisonidazole ([^{18}F]FMISO) was the first specific hypoxia PET tracer and, although it may be the most frequently used tracer for this purpose, its suitability is limited because of slow tumor-specific accumulation and nonspecific washout (4). Second-generation 2-nitroimidazole tracers with different clearance and hydrophilicity characteristics have been developed in an attempt to overcome these disadvantages, [^{18}F]fluoroazomycin arabinoside (FAZA), [^{18}F]fluoroerythronitroimidazole (FETNIM), and [^{18}F]tri-fluoroetanidazole. In preclinical settings, these tracers have been investigated separately or solely in comparison to hypoxia immunohistochemical staining or [^{18}F]FMISO PET imaging, using different experimental setups, tumor models, and acquisition protocols (5-8). Next, the third-generation hypoxia tracer [^{18}F]flortanidazole (HX4) was developed and evaluated in a preclinical rhabdomyosarcoma tumor model, where it was found to be dependent on tumoral oxygenation status (9). Only recently, a comparative study in preclinical animal models reported a clear relationship among the uptake of [^{18}F]FMISO, [^{18}F]FAZA, and [^{18}F]HX4 and with immunohistochemical staining for perfusion, hypoxia, and carbonic anhydrase IX (10). With respect to usage of PET tumor hypoxia for patient imaging, clinical studies have indicated that both [^{18}F]FAZA and [^{18}F]FMISO have prognostic potential (11, 12), and a phase 1 clinical study demonstrated that imaging using [^{18}F]HX4 was feasible and nontoxic (13).

In this study, we compared the 3 most frequently used and clinically available hypoxia tracers, [^{18}F]FMISO, [^{18}F]FAZA, and [^{18}F]HX4, along with the metabolic tracer [^{18}F]fluorodeoxyglucose (FDG) in a preclinical tumor model. We investigated the uptake of each tracer over time and determined the tumor-to-background ratios. A second PET scan was performed on the same animal after 48 hours to assess spatial reproducibility. Furthermore, tracer uptake was challenged by exposing the animals to modified oxygen concentrations. The focus of this study was to investigate the performance and characteristics of the different hypoxia PET tracers, using the same tumor model.

Methods and Materials

Tracer synthesis, tumor model, experimental design

Tracer synthesis of [^{18}F]FMISO, [^{18}F]FAZA, and [^{18}F]HX4 (Fig. 1A) was performed as described previously (14-17). All animal experimental procedures were approved by the Animal Ethical Committee of Maastricht University and were in accordance with the Helsinki Declaration of 1975, as revised in 2000. Adult WAG/Rij rats received subcutaneous implants of syngeneic rhabdomyosarcoma R1 tumors (1 mm^3) in the lateral flank. Experiments were started when tumors reached a minimal volume of 3 cm^3 to meet the resolution of the PET scanner and to have a stable hypoxic (18) and necrotic (5) area. Average tumor volume for [^{18}F]FDG was 21 ± 12 cm^3, 16 ± 6 cm^3 for [^{18}F]FAZA, 13 ± 6 cm^3 for [^{18}F]FMISO, and 11 ± 5 cm^3 for [^{18}F]HX4. During the experimental procedures, rats were anesthetized with intraperitoneal injections of sodium pentobarbital (60 mg/kg). Animals were immobilized on a board and placed outside the scanner between scans to maintain and monitor anesthesia. Radioactive tracers (radiochemical purity was maintained at >95% and synthesis yield at 5.2 ± 2.5 GBq) were injected into the lateral tail vein by using an intravenous line (0.4 mm 27-G Venoflux needle; Vygon Vet, Ecouen, France) flushed with 10% heparin solution (21 ± 2 MBq for [^{18}F]FDG, 17 ± 5 MBq for [^{18}F]FAZA, 21 ± 2 MBq for [^{18}F]FMISO, and 21 ± 2 MBq for [^{18}F]HX4).

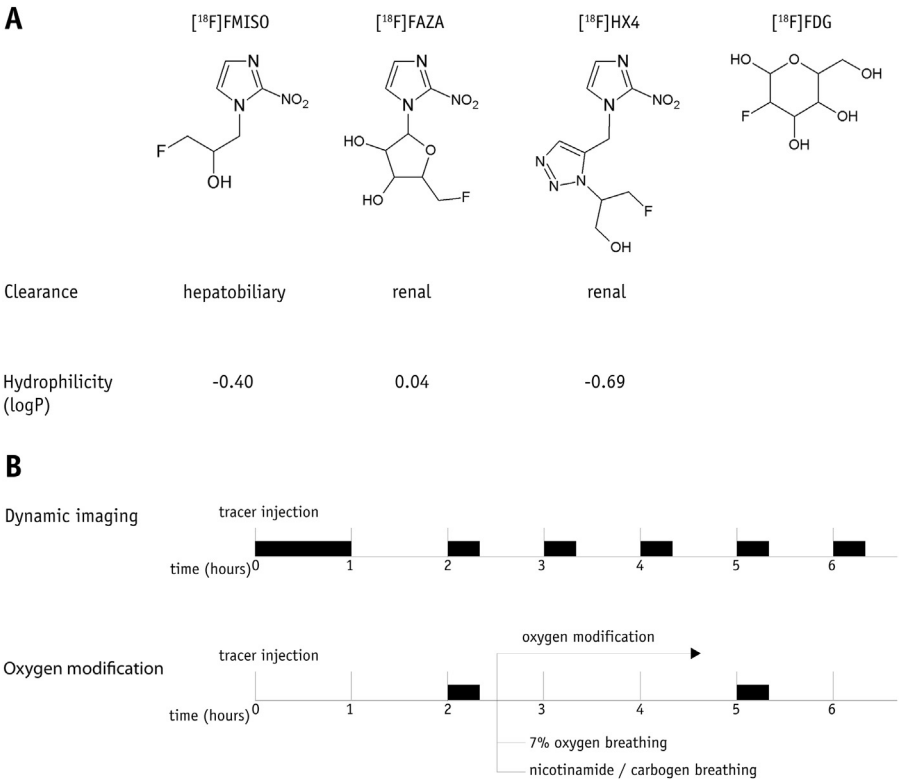

Fig. 1. Tracer characteristics and imaging protocols. (A) Structure formula, main clearance system, and logP values for hydrophilicity of the 3 hypoxia tracers [^{18}F]FMISO, [^{18}F]FAZA, and [^{18}F]HX4 and the metabolic tracer [^{18}F]FDG [9]. (B) Schematic representation of the different imaging protocols for dynamic imaging and for oxygen modification, using either nicotinamide combined with carbogen breathing or 7% oxygen breathing. Imaging acquisition is indicated by black boxes.

Image acquisition and analysis

Images were acquired and analyzed using a clinical PET/CT scanner (Siemens Biograph 40; Siemens Healthcare) and dedicated software (TrueD VC60; Siemens) as described in more detail in online supplementary material (available online at www.redjournal.com) and previously (9). Tumor-to-blood ratios (TBR) and tumor-to-muscle ratios (TMR) were determined using heart and muscle of the hind leg as background tissue, respectively. Spatial reproducibility scans were performed in the same animal within short time frames, using rigid registration voxel-to-voxel analysis (from 2 to 6 hours post injection [p.i.]) or 48 hours apart using nonrigid registration (see supplementary material; available online at www.redjournal.com) of the tumor for long-term comparison to overcome the 24% tumor growth (which were 31% ± 2% for [^{18}F]FDG, 26% ± 2% for [^{18}F]FAZA, 23% ± 1% for [^{18}F]FMISO, and 22% ± 3% for [^{18}F]HX4). Furthermore, a voxel-wise comparison of the 2 scans was performed for which a correlation coefficient was calculated. Imaging schedules for oxygen modification using either nicotinamide (500 mg/kg, intraperitoneal) and carbogen (95% O_2, 5% CO_2; flow = 5 L/min) or 7% oxygen (residual N_2 flow = 2.5 L/min) breathing are shown in Figure 1B. In short, after injection of the tracer, the first basal scan was performed at 2 hours p.i., followed by oxygen modification treatment and a second scan at 5 hours p.i.

Statistics

Prism version 5.01 software (GraphPad) for Windows (Microsoft) was used to perform statistical analyses. To determine the statistical significance of differences between 2 independent groups of variables, we used the nonparametric Mann-Whitney *U* test for small groups. Spatial reproducibility was analyzed using either a Dice similarity coefficient for the calculation of the overlap fractions or Pearson correlation for voxel comparison. *P* values of $<.05$ were assumed to be significant.

Results

PET/CT imaging was performed to assess tracer accumulation over time for the 4 different tracers, using a dynamic imaging schedule (Fig. 1 A and B). Each tracer had a different accumulation pattern within the tumor, represented by maximum (SUV_{max}; Fig. 2A) and mean (SUV_{mean}; Fig. E1A; available online at www.redjournal.com) standardized uptake values, whereas blood and muscle tracer uptake exhibited similar patterns. Due to clearance of the

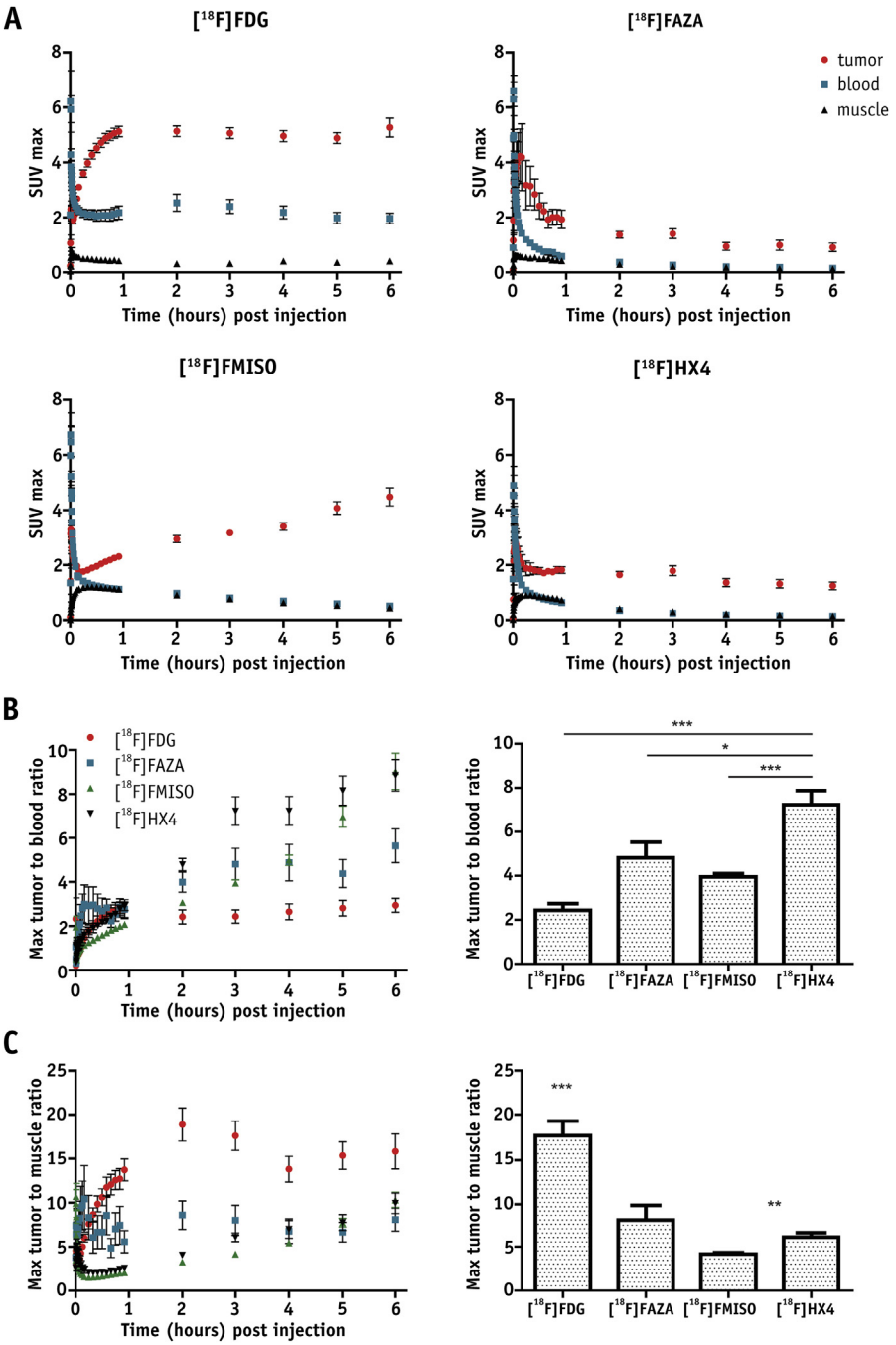

Fig. 2. SUV_{max} and TBR. (A) SUV_{max} of the tumor (red), blood (blue), and muscle (black) over time. (B [Left]) Maximum TBR over time for [^{18}F]FDG (red), [^{18}F]FAZA (blue), [^{18}F]FMISO (green), and [^{18}F]HX4 (black). (B [Right]) TBR tracer comparison at 3 hours p.i. *P<.05, ***P<.001. (C [Left]) Maximum TMR over time. (C [Right]) Maximum TMR comparison for the 4 tracers at 3 hours p.i. Number of animals for all experiments: [^{18}F]FDG n = 12, [^{18}F]FAZA n = 12, [^{18}F]FMISO n = 16, and [^{18}F]HX4 n = 18 except for Figure C [^{18}F]FAZA n = 12. Data are means ± SEM. SUV_{max} = maximum standard uptake value; TBR = tumor-to-blood ratio; TMR = tumor-to-muscle ratio. A color version of this figure is available at www.redjournal.org.

nonspecific binding and specific trapping in hypoxic tumor regions, all TBRs were greater than 1 (Fig. 2B and Fig. E1B; available online at www.redjournal.com). Furthermore, clearance rates for heart and muscle were comparable, giving a muscle to blood ratio around unity (Fig. E1D; available online at www.redjournal.com). For the metabolic tracer [^{18}F]FDG, the maximal TBR of 2.4 ± 0.3 was reached at 2 hours p.i. Of all the hypoxia tracers, [^{18}F]FAZA was the first to reach a plateau phase for TBR at 2 hours p.i. (4.0 ± 0.5), followed by [^{18}F]HX4 (7.2 ± 0.7) at 3 hours p.i. (Fig. 2B). TBR for [^{18}F]FMISO kept increasing; TBR of [^{18}F]FMISO at 6 hours p.i. was comparable to that of [^{18}F]HX4 at 3 hours

p.i. At the first stable time point for [^{18}F]HX4 (3 hours p.i.), this tracer had a significantly higher TBR than either [^{18}F]FAZA ($P = .0154$) or [^{18}F]FMISO ($P < .0001$) (Fig. 2B, right panel); even at 2 hours p.i., [^{18}F]HX4 had already reached a TBR that was equal to or higher than that of [^{18}F]FMISO or [^{18}F]FAZA. When muscle tissue was used as a reference, trends were shown for the hypoxia tracers that were similar compared to maximal TBR (Fig. 2C and Fig. E1C; available online at www.redjournal.com).

Uptake images from 2, 3, 4, and 5 hours p.i. were compared to the 6-hour p.i. scan to perform a voxel-to-voxel comparison of absolute tumor uptake. A correlation coefficient was calculated from the 2 scans (Fig. 3A). Averaged correlation coefficients demonstrated a stable uptake pattern in the tumor for all investigated tracers over short time periods (up to 6 hours) (Fig. 3B). Reproducibility was studied by comparing 2 PET scans acquired within a 48-hour time interval using voxel-to-voxel analyses. Calculated correlation coefficients were high for [^{18}F]FDG (0.87), [^{18}F]FMISO (0.86), and [^{18}F]HX4 (0.76); whereas [^{18}F]FAZA had a significantly ($P < .05$) lower correlation coefficient (0.52) (Fig. 3C). To further investigate spatial reproducibility, we calculated an overall Dice similarity coefficient in which the high uptake region as a percentage of the total tumor volume from the first scan was compared to the same percentage of total volume area from a second scan (Fig. 3D). This analysis showed a high reproducibility for [^{18}F]FDG (0.83), [^{18}F]FMISO (0.85), [^{18}F]HX4 (0.79), and

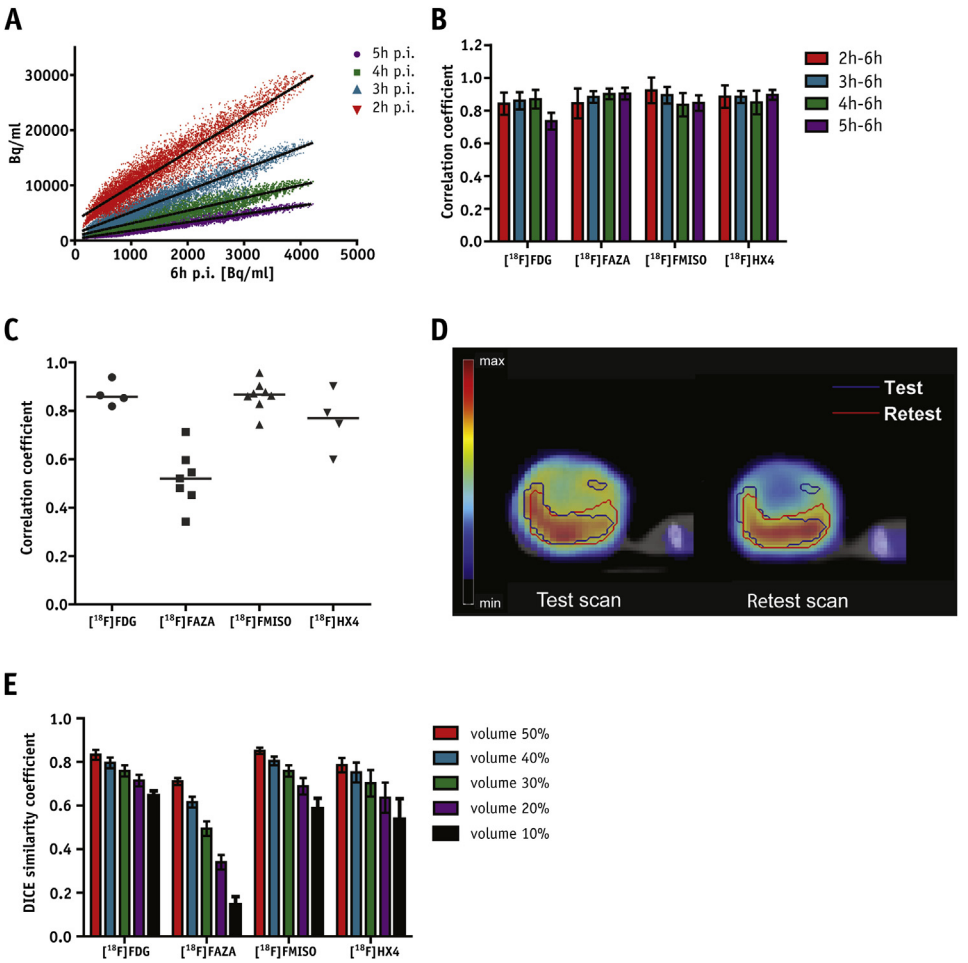

Fig. 3. Voxel-to-voxel analysis and spatial reproducibility. (A) Dynamic scans were used for voxel-to-voxel comparison between the scan obtained at 2, 3, 4, or 5 hours p.i. and the 6-hour scan, shown in the representative scatter plot. (B) Correlation coefficients of voxel-to-voxel analyses over a short-term time frame. For all tracers, n = 4. (C) Correlation coefficients of voxel-to-voxel analyses over a 48-hour time frame shows [^{18}F]FAZA is significantly lower: $P_{FDG\ vs\ FAZA} = 0.0061$, $P_{FAZA\ vs\ FMISO} = 0.0003$, and $P_{FAZA\ vs\ HX4} = 0.0121$. Each dot represents 1 animal, and the mean is indicated. (D) Representative [^{18}F]HX4 PET/CT image of a tumor cross-section visualized over a 48-hour interval. Delineation on the test and retest scans shows the 30% of the total tumor volume with the highest SUV. Overlapping fractions of these regions were calculated and represent the Dice similarity coefficient. (E) Spatial reproducibility over a 48-hour time frame is presented per tracer as a percentage of total tumor volume: [^{18}F]FDG n = 4, [^{18}F]FAZA n = 7, [^{18}F]FMISO n = 8, and [^{18}F]HX4 n = 4. Data are means ± SEM.

[^{18}F]FAZA (0.71) in a comparison of the 50% tumor volume with the highest tracer uptake. However, when only the 10% highest uptake of the tumor volume was selected, [^{18}F]FDG, [^{18}F]FMISO, and [^{18}F]HX4 showed high spatial reproducibility (0.65, 0.59, and 0.49, respectively), whereas [^{18}F]FAZA showed a significantly lower ($P<.05$) spatial reproducibility of 0.14 (Fig. 3E).

Rats were exposed to 7% oxygen breathing (Fig. 1B), mimicking acute hypoxia. The relative SUV_{mean} tracer uptake after 7% oxygen treatment was significantly increased for [^{18}F]HX4 ($P<.01$) and [^{18}F]FAZA ($P<.05$) in the tumor compared to that in untreated animals (Fig. 4A). The mean TBR for [^{18}F]FAZA was significantly increased ($P<.05$); the mean TMR showed a significant increase for all 3 hypoxia tracers ([^{18}F]FAZA, $P<.01$; [^{18}F]FMISO, $P<.05$; and [^{18}F]HX4, $P<.01$) (Fig. 4A). When the effect of maximal tumor uptake on increased hypoxia was studied, no significant effects were observed, although there was a trend toward increased uptake of [^{18}F]HX4 in the tumor (Fig. E2A; available online at www.redjournal.com).

The reversibility of tracer uptake on tumor reoxygenation was examined by treating the rats with nicotinamide

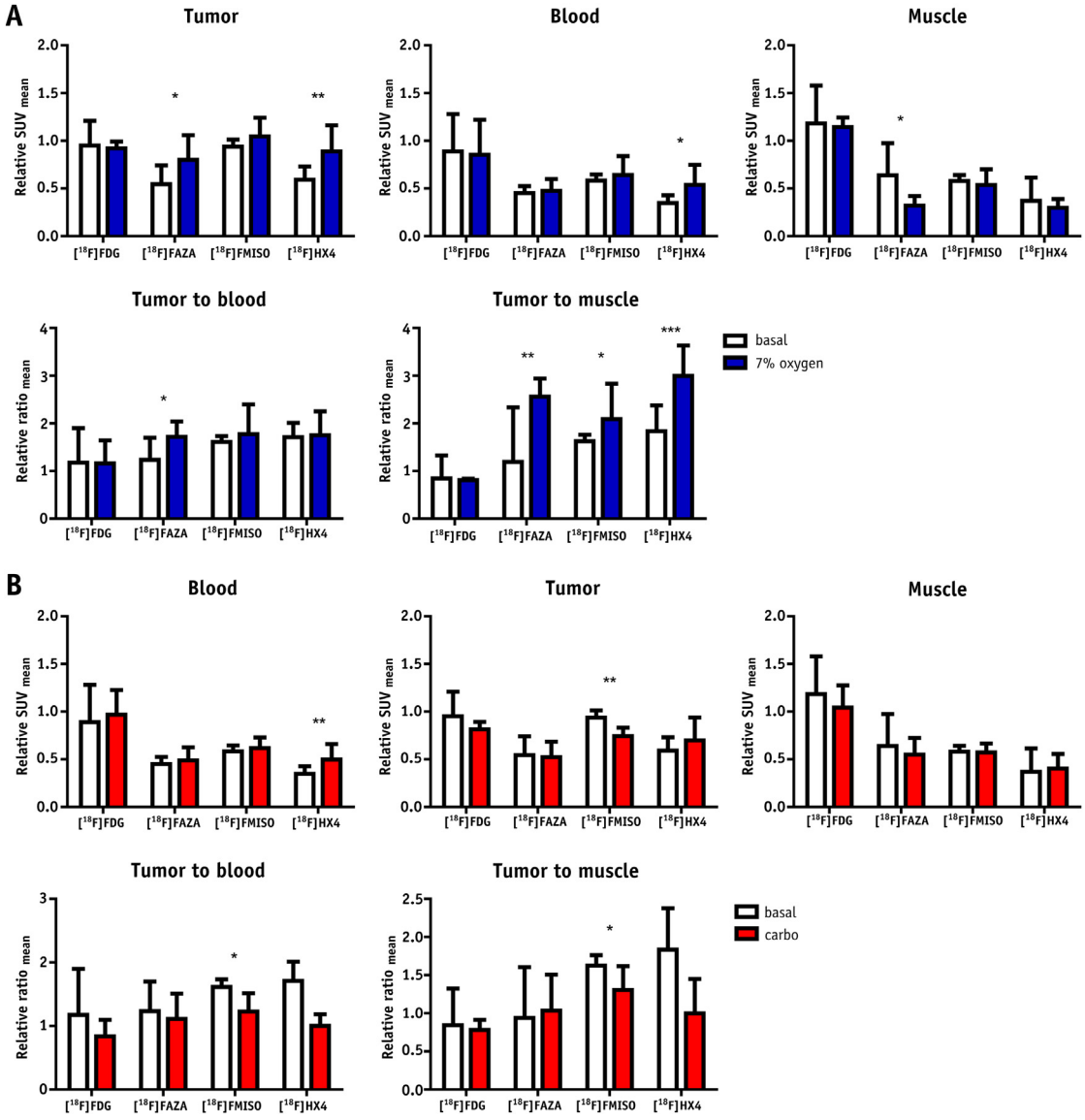

Fig. 4. Oxygen modification. Relative SUV_{mean} and tracer ratios compare untreated rats (basal) with those breathing 7% oxygen (7% oxygen) (A) and those receiving nicotinamide/carbogen (carbo) treatment (B). SUVs were calculated and compared 5 hours p.i. to 2 hours p.i. (vertical axis: relative SUV) for each organ separately and for the relative TBR or TMR at 5 hours p.i. compared to 2 hours p.i. *$P<.05$, **$P<.01$, ***$P<.001$. Data are means ± SD for basal: [^{18}F]FDG n = 12, [^{18}F]FAZA n = 14, [^{18}F]FMISO n = 16, and [^{18}F]HX4 n = 18; for 7% oxygen: [^{18}F]FDG n = 7, [^{18}F]FAZA n = 7, [^{18}F]FMISO n = 8, and [^{18}F]HX4 n = 8; for carbo: [^{18}F]FDG n = 8, [^{18}F]FAZA n = 8, [^{18}F]FMISO n = 6, and [^{18}F]HX4 n = 14. p.i. = post injection; SUV_{max} = maximum standard uptake value; TBR = tumor-to-blood ratio; TMR = tumor-to-muscle ratio.

and carbogen (Fig. 1B). Relative SUV_{mean} (Fig. E1A; available online at www.redjournal.com) indicated that [^{18}F]FMISO remained stable over time in the baseline situation, whereas for other tracers uptake decreased. Influencing tumors toward a more oxygenated state only caused a decrease in [^{18}F]FMISO tumor uptake and did not change uptake of [^{18}F]HX4 and [^{18}F]FAZA (Fig. 4B). Blood uptake values increased for [^{18}F]HX4, but uptake in the muscle was not influenced. Mean TBR and TMR significantly decreased for [^{18}F]FMISO, and maximal values demonstrated comparable results (Fig. E2B; available online at www.redjournal.com).

Discussion

This study compared the frequently used hypoxia PET tracers [^{18}F]FMISO, [^{18}F]FAZA, and [^{18}F]HX4 and the metabolic tracer [^{18}F]FDG in an animal tumor model to assess their tumor-to-background ratios, spatial reproducibility, and sensitivity to oxygen modification.

The rat rhabdomyosarcoma R1 model with a large hypoxic fraction (18) was chosen to ensure sufficient visualization of the uptake of hypoxia tracers using a preclinical model on a clinical PET/CT scanner. Although some variation in tumor volume was seen, the hypoxic fraction was shown to be stable within the tumor model (18). PET acquisition was performed from the time of injection until 6 hours p.i. to determine the optimal uptake in the tumor and highest TBR. In this study, we found the most optimal TBR for [^{18}F]FAZA at 2 hours p.i. This finding is consistent with clinical studies in head and neck squamous cell carcinoma and non−small-cell lung cancer (NSCLC), where imaging at 4 hours p.i. did not improve the TBR compared to 2 hours p.i. (19-21). [^{18}F]HX4 showed an optimal TBR at 3 hours p.i., which was also observed in an NSCLC patient study where image contrast did improve from 2 to 4 hours p.i. (22). As clinically demonstrated, [^{18}F]FMISO does not show plateau formation and has better TBR at later time points (23), which was also observed in this preclinical study. Comparative studies already have indicated that [^{18}F]HX4 imaging in head and neck cancer patients at 1.5 hours p.i. was found to have TMR properties similar to those of [^{18}F]FMISO at 2 hours p.i. (24). This is also reflected in the biological half-life of the tracers, which is much higher in normal tissue for [^{18}F]FMISO (clinical: 12-13 hours [22]; preclinical: 4.5 hours) than for [^{18}F]HX4 (clinical: 4.3 hours [22]; preclinical: 2.2 hours) or [^{18}F]FAZA (preclinical: 2.8 hours). The findings from this preclinical study are in line with those from available clinical studies, and although caution needs to be taken in extrapolation of the data, this might indicate that the results found here in this animal model can be translated to some extent to the clinical setting.

One disparity between clinical and preclinical studies is the use of anesthetic drugs. In this study, pentobarbital was used, and although it was shown that this causes a reduction in the radioactivity in blood and muscle, it did not influence tracer uptake in the tumor, nor did it lead to a significant change in tumor-to-background ratios (25).

The ultimate goal of tumor hypoxia imaging is to improve treatment outcome either by detecting hypoxia to aid in the decision to add specific antihypoxia drugs or by adapting radiation therapy using image guidance. Considering that hypoxia imaging can be used to generate personalized intensity modulated radiation therapy plans in which these radiation-resistant parts of the tumor can be boosted (26, 27), it would be desirable to have a tracer that shows stable uptake over time so that a single scan could be used for several days of treatment. Voxel-to-voxel analyses resulted in high reproducibility for all tracers within a 6-hour scan. Examining spatial reproducibility by comparing a high uptake region revealed good overlap between 2 consecutive scans 48 hours apart for [^{18}F]FMISO, [^{18}F]HX4, and [^{18}F]FDG. For [^{18}F]FMISO, this was also reported in a recent clinical head and neck patient study in which 2 scans were highly reproducible over 48 hours (28). However, voxel-to-voxel analysis of [^{18}F]FMISO uptake over a 3-day interval found a correlation of the hypoxic distribution in less than 50% of the head and neck cancer patients (29). [^{18}F]FMISO in the same patient population and during chemoradiation therapy showed a stable conformation of the hypoxic subvolumes (30). Our data show that reproducibility of [^{18}F]FAZA is poor after 48 hours, even without additional anticancer treatment. This is surprising given the fact that all investigated hypoxia tracers are based on the same nitroimidazole trapping mechanism. Contradictions in [^{18}F]FAZA reproducibility are observed between different preclinical and clinical studies, which might also be caused by the differences in metabolism among organisms. Preclinical microPET analysis of [^{18}F]FAZA uptake showed voxel-to-voxel reproducibility between 2 baseline scans performed 24 hours apart; even after fractionated radiation therapy, a fairly stable intratumoral tracer distribution was observed (31). However, in a clinical trial, [^{18}F]FAZA uptake was evaluated after several rounds of radiation therapy treatment and hypoxic regions were found not to be in the same location (19). Although [^{18}F]HX4 shows good reproducibility in first clinical experiments (22), the stability of [^{18}F]HX4 in detecting the hypoxic fraction during therapy needs to be further assessed. Uptake of [^{18}F]FDG was clearly distinguishable from background and was highly reproducible, demonstrating the outstanding application of [^{18}F]FDG in the detection of tumors. However, we consider [^{18}F]FDG to be a metabolic tracer rather than a marker for hypoxia.

Because tumor hypoxia is a dynamic process that consists of both chronic and acute hypoxia, a tumor's oxygen status changes continuously, and most hypoxia tracers mainly detect the chronic hypoxic fraction. However, there are suggestions that acute hypoxia also plays a prominent role in determining the treatment outcome (32). Changing a

tumor's oxygen status by clamping or reduced oxygen breathing mimics this dynamic process and gives the opportunity to study the behavior of tracer uptake under these conditions. In the ideal situation, one would wish a hypoxia tracer to rapidly and specifically accumulate in the hypoxic regions with fast clearance in the nonhypoxic tissues. Binding of the tracer would be irreversible, and no circulating free available tracer would be present.

Previous studies have shown that a treatment combining nicotinamide and carbogen increases a tumor's oxygen status (9, 33), whereas 7% oxygen breathing increases the hypoxic fraction (9). In this study, the oxygen modification was applied only 2.5 hours after tracer injection. Increasing the hypoxic fraction during tracer accumulation is dependent on the presence of unbound, circulating tracer. For all hypoxia tracers, circulating tracer was present after 3 hours, based on the measured activity in the blood (SUV of 2.4 for [^{18}F]FDG; 0.3 for [^{18}F]FAZA; 0.8 for [^{18}F]FMISO; and 0.3 for [^{18}F]HX4); however only [^{18}F]FAZA and [^{18}F]HX4 showed increased uptake in the tumor after 7% oxygen breathing. This effect was observed mainly in the mean values rather than in the maximum values, indicating that the tumor's overall oxygenation was altered, whereas the maximum value is determined by the severe hypoxic regions that will be less affected by this treatment. Exposure to high oxygen concentrations at 2.5 hours after tracer injection would prevent further accumulation or reverse tracer binding. For [^{18}F]FAZA, preclinical data are available that show reduced uptake after pure oxygen or carbogen breathing in tumor-bearing mice (8, 34). In our experimental setting only [^{18}F]FMISO showed a lower uptake upon reduced hypoxia. Together with the results of constant accumulation of [^{18}F]FMISO in the tumor over time these data suggest that further accumulation is prevented when reducing the hypoxic fraction. Previous studies observed that [^{18}F]FMISO uptake in squamous cell carcinoma-bearing mice was influenced by the altered breathing condition (35). These experiments challenged the tracers to their limits and tried to mimic the changing oxygen concentrations in a tumor. It must be kept in mind that these results are influenced by the tumor and animal model chosen and that the tracer metabolism is different in patients. Furthermore, exposing animals to modified oxygen concentration will introduce changes to the whole organism that might influence the distribution and metabolism of the tracer. Our data suggest that [^{18}F]HX4 and [^{18}F]FAZA are more sensitive to acute hypoxia, whereas [^{18}F]FMISO uptake is influenced by reoxygenation.

Conclusions

In conclusion, all investigated tracers showed different characteristics. The ultimate hypoxia tracer has not been developed, but this and other studies show that hypoxia imaging using the existing tracers gives extra information that can be very useful in the treatment of cancer patients.

References

1. Hammond EM, Asselin MC, Forster D, et al. The meaning, measurement and modification of hypoxia in the laboratory and the clinic. *Clin Oncol (R Coll Radiol)* 2014;26:277-288.
2. Horsman MR, Mortensen LS, Petersen JB, et al. Imaging hypoxia to improve radiotherapy outcome. *Nat Rev Clin Oncol* 2012;9:674-687.
3. Brown JM, Giaccia AJ. The unique physiology of solid tumors: Opportunities (and problems) for cancer therapy. *Cancer Res* 1998;58:1408-1416.
4. Krohn KA, Link JM, Mason RP. Molecular imaging of hypoxia. *J Nucl Med* 2008;49(suppl 2):129S-148S.
5. Dubois L, Landuyt W, Cloetens L, et al. [^{18}f]ef3 is not superior to [^{18}f]fmiso for pet-based hypoxia evaluation as measured in a rat rhabdomyosarcoma tumour model. *Eur J Nucl Med Mol Imaging* 2009;36:209-218.
6. Gronroos T, Bentzen L, Marjamaki P, et al. Comparison of the biodistribution of two hypoxia markers [^{18}F]FETNIM and [^{18}F]FMISO in an experimental mammary carcinoma. *Eur J Nucl Med Mol Imaging* 2004;31:513-520.
7. Mahy P, De Bast M, de Groot T, et al. Comparative pharmacokinetics, biodistribution, metabolism and hypoxia-dependent uptake of [^{18}F]-EF3 and [^{18}F]-MISO in rodent tumor models. *Radiother Oncol* 2008;89:353-360.
8. Reischl G, Dorow DS, Cullinane C, et al. Imaging of tumor hypoxia with [^{124}I]IAZA in comparison with [^{18}F]FMISO and [^{18}F]FAZA—First small animal PET results. *J Pharm Pharm Sci* 2007;10:203-211.
9. Dubois LJ, Lieuwes NG, Janssen MH, et al. Preclinical evaluation and validation of [^{18}f]hx4, a promising hypoxia marker for pet imaging. *Proc Natl Acad Sci USA* 2011;108:14620-14625.
10. Carlin S, Zhang H, Reese M, et al. A comparison of the imaging characteristics and microregional distribution of 4 hypoxia PET tracers. *J Nucl Med* 2014;55:515-521.
11. Eschmann SM, Paulsen F, Reimold M, et al. Prognostic impact of hypoxia imaging with 18f-misonidazole PET in non-small cell lung cancer and head and neck cancer before radiotherapy. *J Nucl Med* 2005;46:253-260.
12. Mortensen LS, Johansen J, Kallehauge J, et al. FAZA PET/CT hypoxia imaging in patients with squamous cell carcinoma of the head and neck treated with radiotherapy: Results from the DAHANCA 24 trial. *Radiother Oncol* 2012;105:14-20.
13. van Loon J, Janssen MH, Ollers M, et al. Pet imaging of hypoxia using [^{18}f]hx4: A phase i trial. *Eur J Nucl Med Mol Imaging* 2010;37:1663-1668.
14. Doss M, Zhang JJ, Belanger MJ, et al. Biodistribution and radiation dosimetry of the hypoxia marker ^{18}F-HX4 in monkeys and humans determined by using whole-body PET/CT. *Nucl Med Commun* 2010;31:1016-1024.
15. Lim JL, Berridge MS. An efficient radiosynthesis of [^{18}F]fluoromisonidazole. *Appl Radiat Isot* 1993;44:1085-1091.
16. Reischl G, Ehrlichmann W, Bieg C, et al. Preparation of the hypoxia imaging PET tracer [^{18}F]FAZA: Reaction parameters and automation. *Appl Radiat Isot* 2005;62:897-901.
17. Walsh JC, Kolb HC. Applications of click chemistry in radiopharmaceutical development. *Chimia (Aarau)* 2010;64:29-33.
18. Dubois L, Landuyt W, Haustermans K, et al. Evaluation of hypoxia in an experimental rat tumour model by [(^{18})f]fluoromisonidazole pet and immunohistochemistry. *Br J Cancer* 2004;91:1947-1954.
19. Servagi-Vernat S, Differding S, Hanin FX, et al. A prospective clinical study of F-FAZA PET-CT hypoxia imaging in head and neck squamous cell carcinoma before and during radiation therapy. *Eur J Nucl Med Mol Imaging* 2014;41:1544-1552.
20. Souvatzoglou M, Grosu AL, Roper B, et al. Tumour hypoxia imaging with [^{18}f]faza PET in head and neck cancer patients: A pilot study. *Eur J Nucl Med Mol Imaging* 2007;34:1566-1575.
21. Trinkaus ME, Blum R, Rischin D, et al. Imaging of hypoxia with 18f-faza PET in patients with locally advanced non-small cell lung

cancer treated with definitive chemoradiotherapy. *J Med Imaging Radiat Oncol* 2013;57:475-481.
22. Zegers CM, van Elmpt W, Wierts R, et al. Hypoxia imaging with [(1)(8)f]hx4 pet in nsclc patients: Defining optimal imaging parameters. *Radiother Oncol* 2013;109:58-64.
23. Abolmaali N, Haase R, Koch A, et al. Two or four hour [^{18}F]FMISO-PET in HNSCC. When is the contrast best? *Nuklearmedizin* 2011;50:22-27.
24. Chen L, Zhang Z, Kolb HC, et al. [^{18}F]HX4 hypoxia imaging with PET/CT in head and neck cancer: A comparison with ^{18}F-FMISO. *Nucl Med Commun* 2012;33:1096-1102.
25. Christian N, Bol A, De Bast M, et al. Determination of tumour hypoxia with the PET tracer [^{18}F]EF3: Improvement of the tumour-to-background ratio in a mouse tumour model. *Eur J Nucl Med Mol Imaging* 2007;34:1348-1354.
26. Hendrickson K, Phillips M, Smith W, et al. Hypoxia imaging with [^{18}F]FMISO-PET in head and neck cancer: Potential for guiding intensity modulated radiation therapy in overcoming hypoxia-induced treatment resistance. *Radiother Oncol* 2011;101:369-375.
27. Thorwarth D, Eschmann SM, Paulsen F, et al. Hypoxia dose painting by numbers: A planning study. *Int J Radiat Oncol Biol Phys* 2007;68:291-300.
28. Okamoto S, Shiga T, Yasuda K, et al. High reproducibility of tumor hypoxia evaluated by ^{18}F-fluoromisonidazole PET for head and neck cancer. *J Nucl Med* 2013;54:201-207.
29. Nehmeh SA, Lee NY, Schroder H, et al. Reproducibility of intratumor distribution of [^{18}F]fluoromisonidazole in head and neck cancer. *Int J Radiat Oncol Biol Phys* 2008;70:235-242.
30. Bittner MI, Wiedenmann N, Bucher S, et al. Exploratory geographical analysis of hypoxic subvolumes using ^{18}F-MISO-PET imaging in patients with head and neck cancer in the course of primary chemoradiotherapy. *Radiother Oncol* 2013;108:511-516.
31. Busk M, Mortensen LS, Nordsmark M, et al. PET hypoxia imaging with FAZA: Reproducibility at baseline and during fractionated radiotherapy in tumour-bearing mice. *Eur J Nucl Med Mol Imaging* 2013;40:186-197.
32. Brown M, Henry S. Kaplan distinguished scientist award lecture 2007. The remarkable yin and yang of tumour hypoxia. *Int J Radiat Biol* 2010;86:907-917.
33. Horsman MR, Overgaard J. Preclinical studies on how to deal with patient intolerance to nicotinamide and carbogen. *Radiother Oncol* 2004;70:301-309.
34. Piert M, Machulla HJ, Picchio M, et al. Hypoxia-specific tumor imaging with ^{18}F-fluoroazomycin arabinoside. *J Nucl Med* 2005;46:106-113.
35. Matsumoto K, Szajek L, Krishna MC, et al. The influence of tumor oxygenation on hypoxia imaging in murine squamous cell carcinoma using [^{64}Cu]Cu-ATSM or [^{18}F]fluoromisonidazole positron emission tomography. *Int J Oncol* 2007;30:873-881.